Article

Structure

Ankyrin Repeats of ANKRA2 Recognize a PxLPxL Motif on the 3M Syndrome Protein CCDC8

Highlights

- The 3M syndrome protein CCDC8 is a top binder of the ankyrin-repeat protein ANKRA2
- ANKRA2 recognizes a PxLPxL motif located at the C-terminal domain of CCDC8
- The N-terminal domain of CCDC8 interacts with two other 3M syndrome proteins
- ANKRA2 binds HDAC4 and HDAC5 to block the interaction with CUL7

Authors

Jianyun Nie, Chao Xu, ..., Tony Pawson, Xiang-Jiao Yang

Correspondence

xiang-jiao.yang@mcgill.ca (X.-J.Y.), jr.min@utoronto.ca (J.M.)

In Brief

The genetic disease 3M syndrome is a rare short-stature disorder with additional features such as facial and skeletal abnormalities. Nie et al. identify a code by which one 3M syndrome protein, CCDC8, interacts with a binding partner, ANKRA2, thereby unveiling an unexpected molecular mechanism important for the pathogenesis of this genetic disease.

Accession Numbers

4LG6
4QQI
3V31
3V2X

Nie et al., 2015, Structure *23*, 700–712
April 7, 2015
http://dx.doi.org/10.1016/j.str.2015.02.001

CellPress

Structure
Article

Ankyrin Repeats of ANKRA2 Recognize a PxLPxL Motif on the 3M Syndrome Protein CCDC8

Jianyun Nie,[1,2,9] Chao Xu,[3,9] Jing Jin,[4,9,10] Juliette A. Aka,[1,9] Wolfram Tempel,[3] Vivian Nguyen,[4] Linya You,[1] Ryan Weist,[1] Jinrong Min,[3,5,*] Tony Pawson,[4,6,11] and Xiang-Jiao Yang[1,7,8,*]

[1]The Rosalind & Morris Goodman Cancer Research Center, Department of Medicine, McGill University, Montréal, QC H3A 1A3, Canada
[2]Department of Breast Cancer, The Third Affiliated Hospital, Kunming Medical University, Yunnan 650118, China
[3]Structural Genomics Consortium, University of Toronto, 101 College Street, Toronto, ON M5G 1L7, Canada
[4]Lunenfeld-tanenbaum Research Institute, Toronto, ON M5G 1X5, Canada
[5]Department of Physiology, University of Toronto, Toronto, ON M5S 1A8, Canada
[6]Department of Molecular Genetics, University of Toronto, Toronto, ON M5G 1L7, Canada
[7]Department of Biochemistry, McGill University, Montréal, QC H3A 1A3, Canada
[8]McGill University Health Center, Montréal, QC H3A 1A3, Canada
[9]Co-first author
[10]Present address: Department of Medicine-Nephrology/Hypertension, Northwestern University, 320 East Superior Street Searle 10-521, Chicago, IL 60611, USA
[11]The author passed away unexpectedly in 2013
*Correspondence: xiang-jiao.yang@mcgill.ca (X.-J.Y.), jr.min@utoronto.ca (J.M.)
http://dx.doi.org/10.1016/j.str.2015.02.001

SUMMARY

Peptide motifs are often used for protein-protein interactions. We have recently demonstrated that ankyrin repeats of ANKRA2 and the paralogous bare lymphocyte syndrome transcription factor RFXANK recognize PxLPxL/I motifs shared by megalin, three histone deacetylases, and RFX5. We show here that that CCDC8 is a major partner of ANKRA2 but not RFXANK in cells. The *CCDC8* gene is mutated in 3M syndrome, a short-stature disorder with additional facial and skeletal abnormalities. Two other genes mutated in this syndrome encode CUL7 and OBSL1. While CUL7 is a ubiquitin ligase and OBSL1 associates with the cytoskeleton, little is known about CCDC8. Binding and structural analyses reveal that the ankyrin repeats of ANKRA2 recognize a PxLPxL motif at the C-terminal region of CCDC8. The N-terminal part interacts with OBSL1 to form a CUL7 ligase complex. These results link ANKRA2 unexpectedly to 3M syndrome and suggest novel regulatory mechanisms for histone deacetylases and RFX7.

INTRODUCTION

Primordial dwarfism comprises heterogeneous diseases that involve diverse molecular and cellular mechanisms (Klingseisen and Jackson, 2011). 3M syndrome is a primordial growth disorder named after three principal scientists (Miller, McKusick, and Malvaux) who first reported this genetic disease four decades ago (Miller et al., 1975). Such patients display prenatal and postnatal growth retardation along with frontal bossing, triangular face, midface hypoplasia, and other distinct facial abnormalities but possess typically normal intelligence, indicating that facial but not brain development is affected (Clayton et al., 2012; Hanson et al., 2011, 2012; Litterman et al., 2011). Growth hormone is often normal in the patients and their response to recombinant growth hormone therapy is variable but typically poor, so the hormone itself may not be the culprit (Clayton et al., 2012). A causal gene was first mapped to chromosome 6p21.1 and found to encode CUL7 (cullin 7) (Huber et al., 2005). A known E3 ubiquitin ligase (Arai et al., 2003; Dias et al., 2002; Furukawa et al., 2003), CUL7 stimulates ubiquitination of p53 (Andrews et al., 2006), insulin receptor substrate (Litterman et al., 2011; Xu et al., 2008), TBC1D3 (TBC1 domain family member 3) (Kong et al., 2012), and hematopoietic progenitor kinase 1 (Wang et al., 2014). Mutations were also found in an unrelated gene encoding OBSL1 (obscurin-like 1), a large protein similar to the N-terminal portion of the giant 720-kDa sarcomeric signaling regulator obscurin (Geisler et al., 2007; Hanson et al., 2009). Two recent studies have discovered mutations on a third gene, *CCDC8* (coiled-coil domain containing 8) (Al-Dosari et al., 2012; Hanson et al., 2011). This gene was so named because its encoded protein contains a putative coiled-coil domain according to bioinformatic analysis (GenBank accession no. Q9H0W5). Due to the mutations in patients with 3M, CUL7, OBSL1, and CCDC8 are considered to function in the same molecular and cellular pathways to regulate protein ubiquitination and control organismal growth (Hanson et al., 2012; Litterman et al., 2011). However, further studies are needed to substantiate this hypothesis and to elucidate the underlying mechanisms.

Ankyrin-repeat family A protein 2 (ANKRA2) contains five ankyrin repeats and was initially identified as a binding partner of megalin, also known as low-density lipoprotein receptor-related protein 2 (LRP2) (Rader et al., 2000). This multiligand receptor is located in the plasma membrane of absorptive epithelial cells to regulate protein uptake from the luminal space (Christensen and Birn, 2002). During yeast two-hybrid screening, ANKRA2 was identified as a binding partner of histone deacetylase 4 (HDAC4) and HDAC5 (McKinsey et al., 2006; Wang et al.,

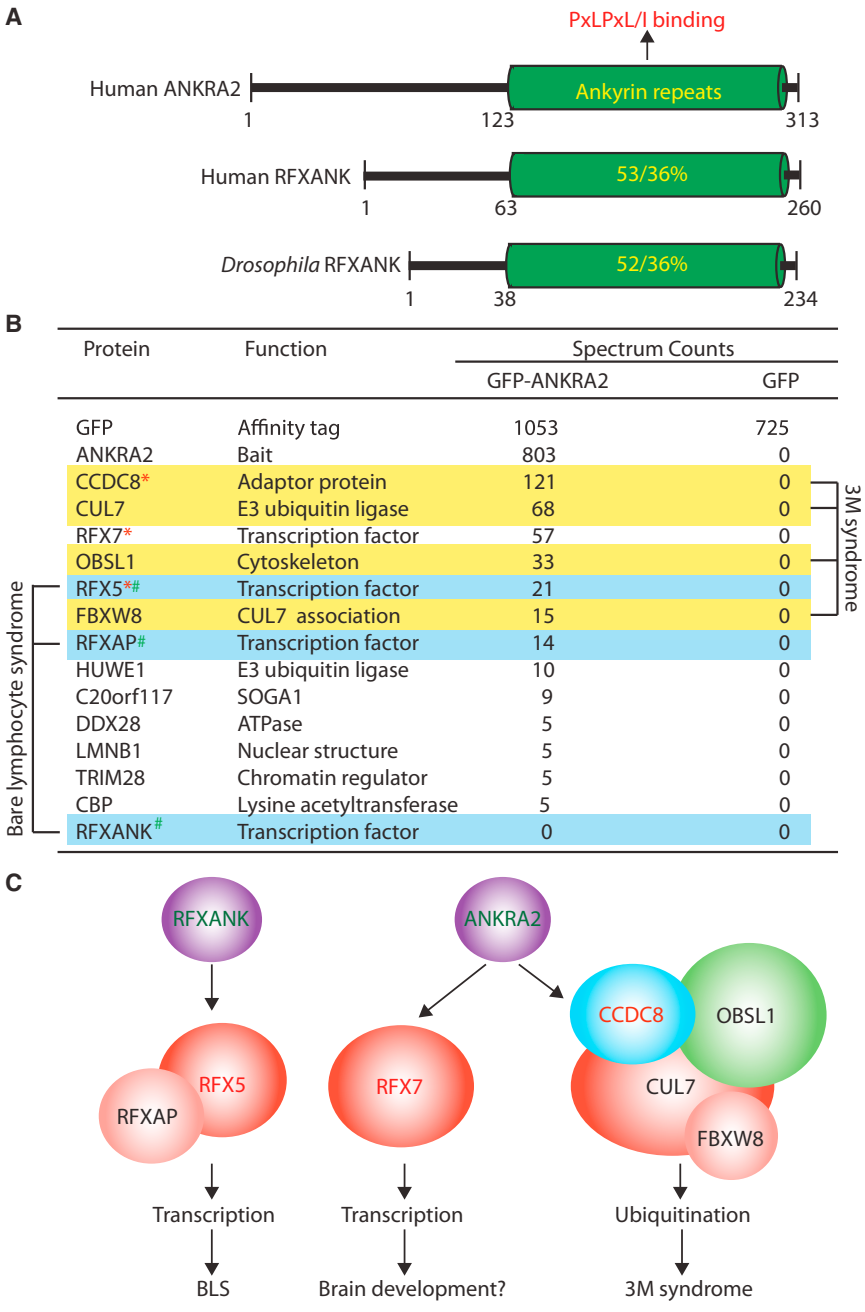

Figure 1. Proteomic Identification of ANKRA2-Interacting Proteins

(A) Schematic representation of human ANKRA2 and RFXANK along with the fly homolog (CG5846, NP_609333). Ankyrin-repeat domains are depicted in green, with sequence similarity and identity toward human ANKRA2 indicated as a percentage. The arrow denotes that ankyrin-repeat domains of human ANKRA2 and RFXANK specifically recognize PxLPxL/I motifs. The *C. elegans* genome does not encode a homologous protein.

(B) List of proteins associated with stably expressed ANKRA2. GFP-ANKRA2 and GFP were stably expressed in HEK293 cells for affinity purification and mass spectrometry. The three proteins linked to 3M syndrome and the F-box protein FBXW8 are highlighted in yellow, while the green number sign (#) labels three proteins associated with BLS. The red asterisk (*) denotes proteins possessing PxLPxL/I motifs.

(C) Cartoons showing how RFXANK and ANKRA2 target RFX7 and two complexes linked to BLS and 3M syndrome. The preference of RFX7 for ANKRA2 is based on binding affinity (see below). See also Figures S1–S3 and Tables S1 and S2.

2005). These two paralogous deacetylases function as transcriptional corepressors to regulate gene expression in the nucleus (Yang and Seto, 2008). Furthermore, the cytoplasmic tail of megalin shares a conserved PxLPxL/I motif with the N-terminal regulatory regions of HDAC4, HDAC5, and perhaps also HDAC9 for specific interaction with ankyrin repeats of ANKRA2 (Xu et al., 2012).

The ankyrin repeats are highly homologous to those of RFXANK (regulator factor X 5 [RFX5]-interacting ankyrin-repeat protein) (Lin et al., 1999; Masternak et al., 1998; Nagarajan et al., 1999; Rader et al., 2000; Xu et al., 2012). Mutations on the *RFXANK* gene are well known to cause the immune disorder bare lymphocyte syndrome (BLS) (Masternak et al., 1998; Nagarajan et al., 1999; Reith and Mach, 2001). RFXANK forms a trimeric transcription factor complex with RFX5 and RFXAP (RFX5-associated protein), encoded by two other genes that are mutated in patients with BLS (Reith and Mach, 2001; Ting and Trowsdale, 2002). This trimeric complex recognizes an enhancer X-box sequence motif, shared by major histocompatibility class II (MHC-II) genes, to recruit the MHC-II transcriptional coactivator CIITA (encoded by the fourth gene mutated in patients with BLS) for activation of gene expression (Reith and Mach, 2001; Ting and Trowsdale, 2002). Similar to the ANKRA2 interaction with megalin and the deacetylases, RFXANK recognizes a PxLPxL motif of RFX5 via its ankyrin-repeat domain (Xu et al., 2012). Therefore, ANKRA2 and RFXANK recognize PxLPxL/I motifs on diverse partners. Despite their sequence and structure similarity, these two ankyrin-repeat proteins display specificity for their partners (Xu et al., 2012). ANKRA2 is more specific for megalin and the deacetylases, whereas RFXANK prefers RFX5 (Xu et al., 2012). Sequences within the PxLPxL/I motifs and the flanking residues dictate this specificity. For example, in RFX5, the methionine preceding the motif and the proline at the +2 position contribute greatly to RFXANK association (Xu et al., 2012). A highly similar ankyrin-repeat domain is present in *Drosophila* but not *Caenorhabditis elegans* (Figure 1A; Figure S1), suggesting that the binding mode is evolutionarily conserved from the fly to humans.

An interesting question is whether there are additional proteins adopting such a mode for interacting with ANKRA2 and RFXANK. Here, we demonstrate that the 3M syndrome protein CCDC8 interacts specifically with ANKRA2 but not with RFXANK. Protein binding and crystal structure analyses confirmed that ANKRA2 recognizes CCDC8 through a PxLPxL motif located at the C-terminal domain. Different from ANKRA2, OBSL1 interacts with the conserved N-terminal domain of CCDC8 to bridge the association with CUL7. In addition, this ligase and ANKRA2 bind to HDAC4 in an antagonistic fashion. These results unravel a previously unappreciated link of ANKRA2 to 3M syndrome and yield new insights into mechanisms whereby HDAC4 and related deacetylases are regulated.

RESULTS

Two Groups of Disease-Causing Partners of ANKRA2 and RFXANK

PxLPxL/I motifs are short sequences present in many proteins. With proper flanking residues, such motifs are sufficient for specific recognition by ANKRA2 and RFXANK (Xu et al., 2012), so an interesting question is whether any new proteins utilize similar motifs for interaction with ANKRA2 or RFXANK. To investigate this, we performed systematic mass spectrometry to identify proteins copurified with ANKRA2 and RFXANK. For this, GFP fusion proteins were expressed for affinity purification on GFP-Trap beads due to their high recovery efficiency (Rothbauer et al., 2008). As listed in Tables S1 and S2, when transiently expressed, GFP-ANKRA2 and -RFXANK coimmunoprecipitated over ten endogenous proteins from HEK293 cell extracts. The proteins were not detected with similar purification with GFP-CRTC2 (CREB-regulated transcription coactivator 2, Tables S1 and S2), indicating that the coimmunoprecipitation (co-IP) is specific. This notion received further support from identification of known partners. Both ANKRA2 and RFXANK coprecipitated RFX5 and RFXAP (Table S1). Notably, RFX5 was recovered as the top partner for RFXANK (Table S2) and one of the top ones for ANKRA2 (Table S1). RFXANK forms a trimeric transcription factor complex with RFX5 and RFXAP (Reith and Mach, 2001; Ting and Trowsdale, 2002) and ANKRA2 may play a similar role (Krawczyk et al., 2005; Long and Boss, 2005). In addition, ANKRA2 coprecipitated HDAC5 (Table S1), which is consistent with the published reports that ANKRA2 interacts with this deacetylase (McKinsey et al., 2006; Wang et al., 2005; Xu et al., 2012). HDAC4 was not identified (Table S1), perhaps due to its low level in the cells used or its regulated interaction with ANKRA2 (Wang et al., 2005; Xu et al., 2012). Among other established partners of ANKRA2, megalin is a membrane-associated receptor whose expression is restricted to the absorptive epithelial cells (Christensen and Birn, 2002; Rader et al., 2000) and may not be present in HEK293 cells. Interestingly, in addition to common binding partners, ANKRA2 and RFXANK coprecipitated distinct proteins (Tables S1 and S2), which is consistent with their distinct preference for partners (Xu et al., 2012). To minimize potential artifacts resulting from transient expression, we stably expressed GFP-ANKRA2 for affinity purification. This strategy recovered a set of proteins (Figure 1B; Figure S2) similar to those from transient expression and affinity purification (Table S1), further supporting the specificity of affinity purification in both strategies.

While RFX5 was identified as the top partner of RFXANK (Table S2), the 3M syndrome protein CCDC8 was recovered unexpectedly as the major partner of ANKRA2 (Figures 1B and 1C; Table S1). CCDC8 did not coprecipitate with RFXANK (Table S2). CCDC8 is a novel protein linked to 3M syndrome (Al-Dosari et al., 2012; Hanson et al., 2011). The other two proteins affected in the syndrome are CUL7 and OBSL1 (Hanson et al., 2009; Huber et al., 2005). Both copurified with ANKRA2 but not with RFXANK (Figure 1B; Tables S1 and S2). Moreover, FBXW8, an F-box protein interacting with CUL7 and regulating its ligase activity (Arai et al., 2003; Dias et al., 2002; Litterman et al., 2011; Xu et al., 2008), copurified with GFP-ANKRA2 (Figure 1B). These results suggest that ANKRA2 forms a complex with CCDC8, OBSL1, CUL7, and FBXW8, four proteins with known roles in 3M syndrome, providing the molecular basis underlying the genetic links to this disease (Figure 1C, right).

Related to RFX5, RFX7 was identified as the second top partner for both ANKRA2 and RFXANK (Figure 1C; Table S1). RFX7 is a poorly characterized protein with a role in breast cancer and may regulate brain development (Aftab et al., 2008; Bae et al., 2014; Yau et al., 2010). Sequence analysis revealed that RFX7 shows high similarity to RFX5 within the N-terminal RFX domains used for DNA binding (Figures S3A–S3C) (Aftab et al., 2008). Importantly, within the RFX domain, there is a PxLPxL motif (Figures S3A–S3C). This motif is conserved in the *Drosophila* homolog of RFX5 and RFX7 (Figures S3A–S3C). The MPxLPxL motif of RFX5 mediates association with RFXANK (Xu et al., 2012), although this may not be the sole surface for RFXANK association (Krawczyk et al., 2005). Interaction of RFX7 with RFXANK or ANKRA2 has not been reported, but the high similarity to RFX5 suggests that RFX7 may utilize its PxLPxL motif to bind ANKRA2 and RFXANK (Figure S3). Thus, along with published reports (Krawczyk et al., 2005; Long and Boss, 2005; Reith and Mach, 2001; Ting and Trowsdale, 2002), these results confirm that RFXANK and ANKRA2 act through RFX5, and perhaps also RFX7, to regulate gene expression (Figure 1C).

In addition to the above two groups of disease-associated proteins (Figure 1C), the E3 ubiquin ligase HUWE1 and the poorly characterized protein C20orf117 (recently named SOGA1 [suppressor of glucose_autophagy associated 1]) copurified with ANKRA2 and RFXANK (Figure 1C; Table S1). Notably, HUWE1 and C20orf117 were also among the top-ranked hits, suggesting their potential functional relevance.

As reported about HDAC4/5/7, RFX5, megalin (Xu et al., 2012), and noted above for RFX7 (Figure S3), an interesting possibility is whether any of the newly identified proteins possess the PxLPxL/I motif. To examine this, we inspected amino acid sequences of the identified candidates. Among all of the proteins newly identified in the mass spectrometric analyses (Figure 1B; Tables S1 and S2), CCDC8 is the only other protein possessing a conserved PxLPxL/I motif (Figure 2A). As described above, CCDC8 was identified as the major partner of ANKRA2 (Figure 1B; Table S1). Because of these two unique features (Figure 2A) and its link to 3M syndrome (Figure 1C) (Al-Dosari et al., 2012; Hanson et al., 2011), we characterized CCDC8 further.

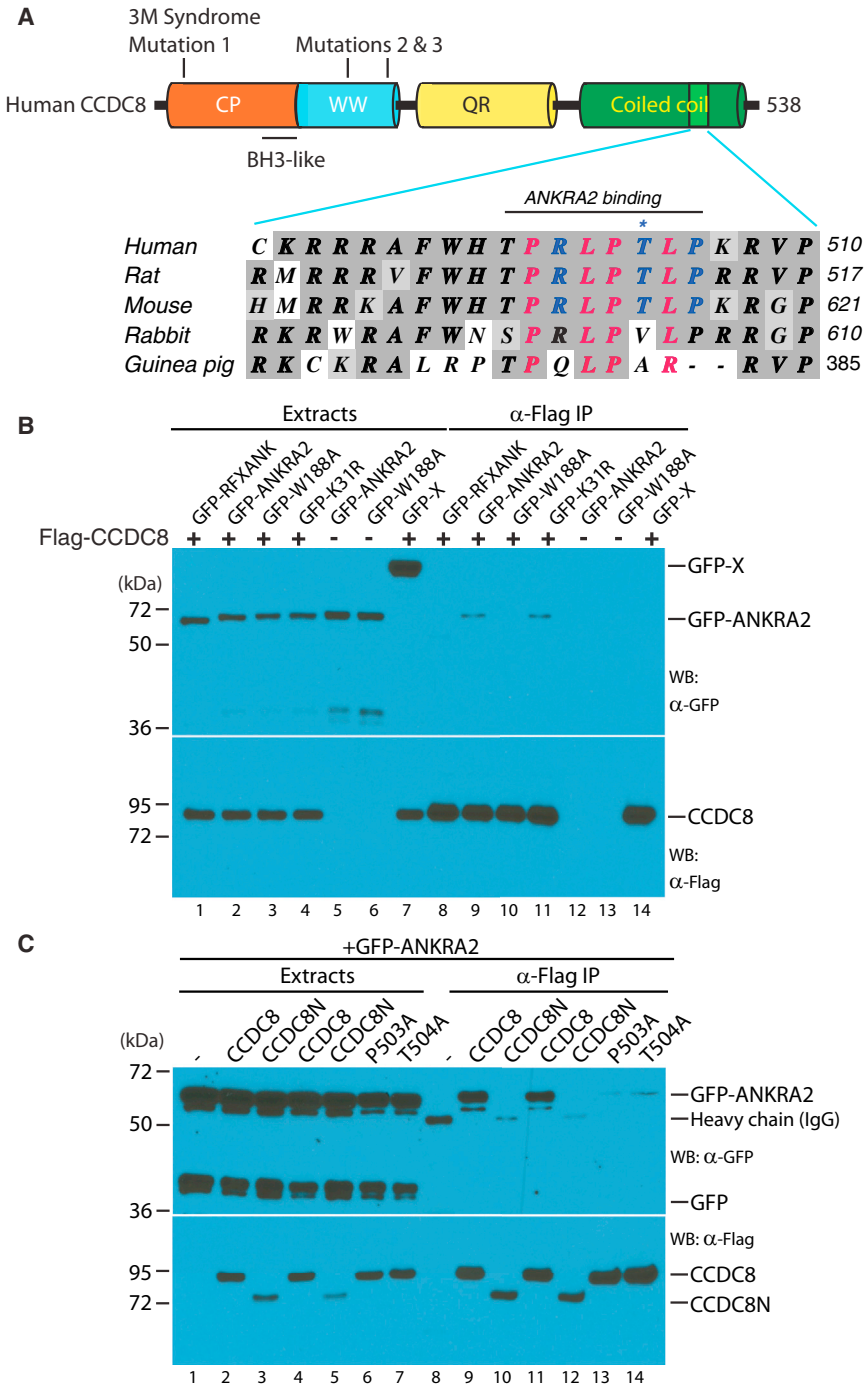

Figure 2. CCDC8 Possesses a PxLPxL Motif for ANKRA2 Interaction

(A) CCDC8 contains highly conserved domains at both ends, with a portion of the N-terminal domain similar to the paraneoplastic Ma antigen (PNMA) family of proteins. This portion, named the CP (CCDC8 and PNMA homologous) domain, harbors a BH3-like motif (Chen and D'Mello, 2010). The region C-terminal to the CP domain is conserved and possesses a putative WW domain. The middle QR domain contains nine AAxxQR repeats, absent in lower mammals such as mice and rats (Figure S4). Embedded within the C-terminal coiled coil is a PxLPxL/R motif, conserved from guinea pig to humans. Positions of thee 3M syndrome-causing mutations are also indicated (Al-Dosari et al., 2012; Hanson et al., 2011).

(B) Co-IP showing that CCDC8 interacts with ANKRA2, but not with its point mutant W188A or with RFXANK. GFP-X, GFP fusion protein of an unrelated protein. Expression vectors for the indicated GFP fusion proteins were separately transfected into HEK293 cells along with the plasmid for Flag-CCDC8 (lanes 1–4, 7, 8–11, and 14) or the corresponding empty vector (lanes 5–6 and 12–13) for affinity purification and immunoblotting.

(C) Co-IP demonstrating that ANKRA2 interacts with CCDC8 but not its C-terminal truncation mutant (CCDC8N) or the point mutants P503A and T504A. See also Figures S4 and S5.

The PxLPxL Motif of CCDC8 Mediates Interaction with ANKRA2

The PxLPxL motif is embedded within the C-terminal domain of CCDC8 and is conserved from mice to humans (Figure 2A; Figure S4). Notably, CCDC8 is specific to mammals and an evolutionarily recent protein, as its orthologs are absent in model organisms such as *Drosophila*, zebrafish, or *Xenopus*. Strikingly, human CCDC8 possesses a QR domain (containing multiple AAxxQR repeats) highly divergent in mouse and rat Ccdc8 (Figure S4). Like the C-terminal domain, the N-terminal domain is highly conserved (Figure 2A; Figure S4). The N-terminal half of the N-terminal domain displays similarity to the N-terminal parts of PNMA (paraneoplastic Ma antigen) proteins, but the functional significance remains elusive. The PNMA family is linked to the paraneoplastic neurological syndrome (Schuller et al., 2005), but the molecular function remains poorly characterized. Some evidence suggests a role in inducing neuronal death through a BH3-like motif (Figure 2A; Figures S5A and S5B) (Chen and D'Mello, 2010).

To analyze interaction between CCDC8 and ANKRA2, we expressed them for co-IP. As shown in Figure 2B, CCDC8 specifically coprecipitated with ANKRA2, supporting their interaction (lanes 2 and 9). This interaction was specific as no such co-IP was detected with RFXANK (lanes 1 and 8). We also analyzed two point mutants of ANKRA2. Mutant K31R affects a putative sumoylation site located outside the ankyrin-repeat domain, whereas mutant W188A impairs interaction with HDAC4 and megalin (Xu et al., 2012). As shown in Figure 2B (lanes 3–4 and 10–11), mutant K31R but not W188A coprecipitated with CCDC8, indicating that CCDC8 adopts a similar mode of interaction with ANKRA2 as HDAC4 and megalin.

We next mapped the ANKRA2 binding site on CCDC8. For this, we analyzed a CCDC8 mutant lacking the C-terminal

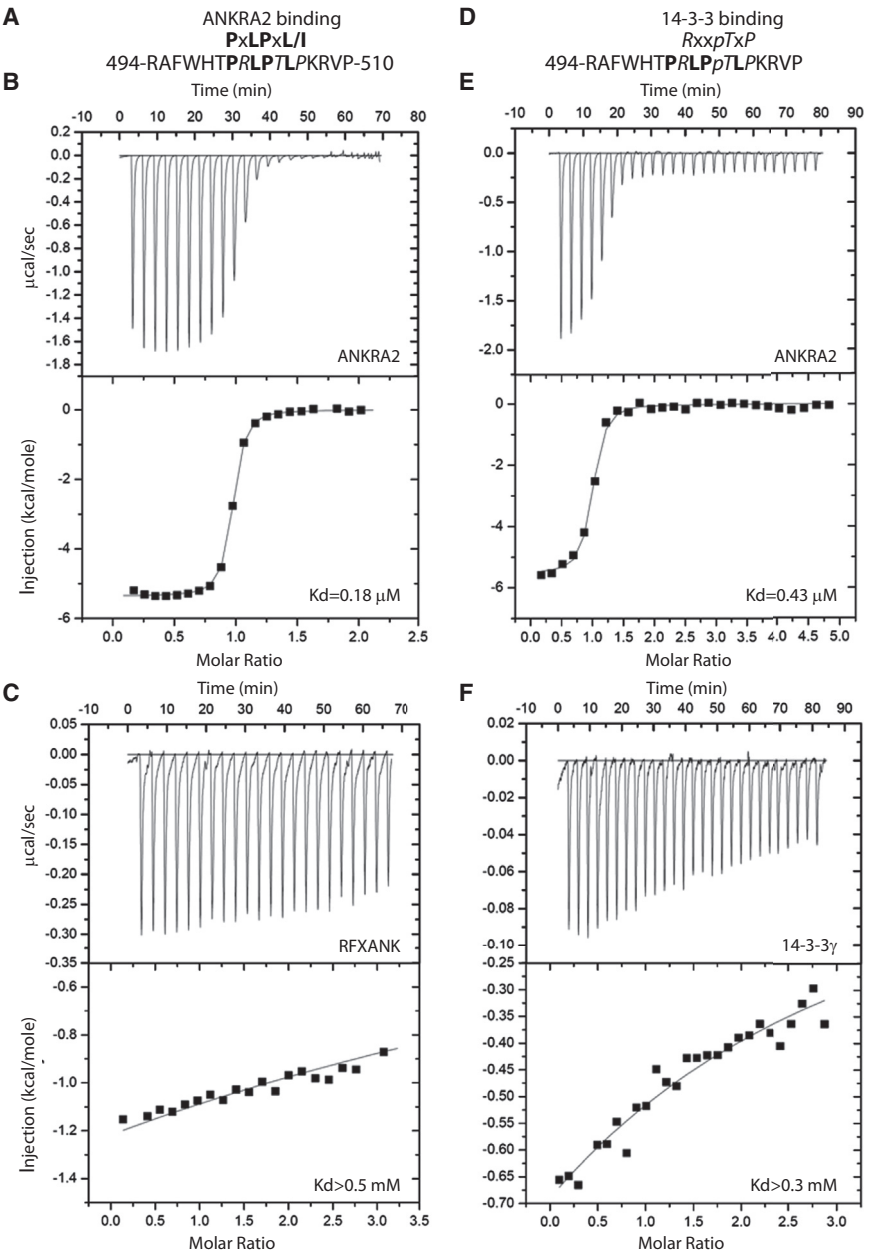

Figure 3. ITC Analysis of the Interaction of CCDC8 Peptides with ANKRA2, RFXANK, and 14-3-3

(A) Amino acid sequence of the unmodified CCDC8 peptide used for ITC analysis. The PxLPxL motif is highlighted in bold and aligned with the consensus sequence for ANKRA2/RFXANK binding, with an RxxTxP motif indicated in italics.

(B and C) ITC measurement of affinities for the ankyrin repeats of ANKRA2 and RFXANK binding toward the unmodified CCDC8 peptide shown in (A).

(D) Amino acid sequence of the phosphorylated CCDC8 peptide used for ITC analysis. The PxLPxL motif is highlighted in bold, and the embedded potential 14-3-3 binding site is aligned with a 14-3-3 binding consensus sequence (in italics).

(E and F) ITC measurement of affinities for the ANKRA2 ankyrin repeats and 14-3-3γ binding to the phosphorylated peptide shown in (D).

coiled-coil domain. As shown in Figure 2C (lanes 1–5 and 7–12), this mutant exhibited much weaker ANKRA2 binding compared with full-length CCDC8, indicating that a major binding site is located at the C-terminal domain. In similar assays, we could not assess whether the C-terminal domain is sufficient for the interaction, as it could not be expressed in the cells (data not shown). To determine whether the PxLPxL motif is necessary for CCDC8 to bind ANKRA2, we engineered two point mutants, P503A and T504A in the 500-PRLPTL-505 sequence. Compared with wild-type CCDC8, P503A displayed much weaker co-IP with ANKRA2 (lanes 6 and 13), confirming the importance of P503 in ANKRA2 association. The T504A mutation also abolished the interaction (lanes 7 and 14), although the reason remains unclear. Together, the results from these co-IP experiments demonstrate that in cells, CCDC8 uses its PxLPxL motif for ANKARA2 interaction.

To determine whether the motif is sufficient for interaction with ANKRA2, we performed isothermal titration calorimetry (ITC) with a peptide corresponding to residues 494–510 of CCDC8 (Figure 3A). As shown in Figure 3B, the peptide bound efficiently to the ankyrin-repeat domain of ANKRA2 with a K_d value of 0.18 µM. By contrast, the binding to the corresponding domain of RFXANK was weak (K_d >500 µM, Figure 3C). As phosphorylation of S350 within the PxLPxL motif of HDAC4 impairs ANKRA2 association (Xu et al., 2012), we wondered whether this is also the case with CCDC8. The corresponding residue in CCDC8 is R501, but T504 is just a few residues away. We thus analyzed the same peptide with T504 replaced with phospho-threonine (Figure 3D). In comparison with the regular peptide, this phosphopeptide exhibited a slightly lower affinity for ANKRA2 (K_d = 0.43 µM versus 0.18 µM, cf. Figures 3E and 3B), indicating that phosphorylation has minimal effects on the binding. T504 constitutes a potential 14-3-3 binding site (Figure 3D) and 14-3-3 may compete with ANKRA2 in binding to the same region. But 14-3-3 exhibited minimal binding to the phosphopeptide (K_d >300 µM, Figure 3F).

The preference of CCDC8 for ANKRA2 over RFXANK is reminiscent of that of HDAC4 and megalin (Figure 4A) (Xu et al., 2012). Notably, the affinity for ANKRA2 was even higher than that of HDAC4, megalin, or RFX7 (Figure 4A; Figure S6), which may explain why it was recovered as the top partner (Figure 1C; Tables S1 and S2). Sequence comparison revealed that the amino acid sequence of the CCDC8 motif is more similar to those of HDAC4, megalin, and RFX7 than to that of RFX5 (Figure 4B),

A

	Kd (μM)		
	ANKRA2	RFXANK	14-3-3γ
CCDC8(494-510)	0.18	>500	ND
CCDC8(pT504)	0.43	ND	>300
HDAC4(343-359)	1.6	109	ND
HDAC4(pS350)	22	ND	9
Megalin(4448-4466)	4.9	ND	ND
RFX5(167-183)	118	184	ND
RFX7(172-188)	3.0	150	ND

B

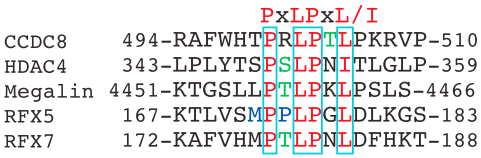

Figure 4. Binding Affinity and Sequence Comparison of Various Known PxLPxL/I Motifs

(A) Summary of the binding affinity of different PxLPxL/I motifs for ANKRA2, RFXANK, and 14-3-3. K_d values for HDAC4, megalin, and RFX5 are derived from a previous report (Xu et al., 2012), whereas the values for CCDC8 and RFX7 are based on ITC analyses performed in this study. ND, not determined. (B) Sequence alignment of known and putative PxLPxL/I motifs. Key residues of the PxLPxL/I motifs are highlighted in red, with the phosphorylatable residues in green and P175 of RFX5 in blue. This residue is key to making RFX5 preferable for RFXANK binding (Xu et al., 2012); because of this proline, the binding pocket of RFXANK receives M173 (also in blue) instead of P174 of RFX5. Although M173 is conserved in RFX7, P175 of RFX5 is replaced with threonine in RFX7. Thus, the core motif of RFX7 is more similar to those of HDAC4 and megalin than to that of RFX5.

reiterating that the PxLPxL/I motif is a prerequisite for the interaction and the sequence at the core motif and the flanking regions contribute to the optimal binding, thereby dictating the preference for ANKRA2 or RFXANK. These results demonstrate that the PxLPxL motif of CCDC8 is efficient in mediating interaction with ANKRA2.

Structural Analysis of ANKRA2 Bound to the PxLPxL Motif of CCDC8

To gain structural insights into ANKRA2 interaction with the motif of CCDC8, we determined the crystal structure of ANKRA2 (residues 142–313, corresponding to the ankyrin-repeat domain; Figure 1A; Figure S1) in complex with CCDC8 (residues 494–510). The complex structure was solved at a resolution of 1.8 Å (Table 1). Only H498-P510 of CCDC8 displayed visible electron density in the costructure. As in the ANKRA2-HDAC4 structure (Xu et al., 2012), the ANKRA2-binding motif (500-PRLPTL-505) of CCDC8 is characteristic of the PxLPxL/I motif from HDAC4 and megalin, making extensive hydrophobic contacts with ankyrin repeats of ANKRA2 (Figure 5; Figure S6). P500 of CCDC8 fits into the hydrophobic pocket formed by F183, W188, A191, H192, and L221 of ANKRA2 (Figure 5; Figure S6). L502 of CCDC8 occupies a second pocket composed of E216, S220, L221, and Y254 of ANKRA2 (Figure 5; Figure S6). P503 of CCDC8 provides additional hydrophobic contact with Y254 and H257 of ANKRA2 (Figure 5; Figure S6). L505 of CCDC8 binds to a third hydrophobic pocket consisting of L291, Y282, H257, and L287 of ANKRA2 (Figure 5; Figure S6). In addition to these four key residues in the ANKRA2-binding motif, T499 near the N terminus of the CCDC8 peptide packs against the rings of F183 and W188 of ANKRA2 (Figure 5; Figures S6 and S7). At the C terminus, P506 of CCDC8 mediates additional hydrophobic interactions with H257, Y282, and L287 of ANKRA2 (Figure 5; Figures S6 and S7). Moreover, the backbone of the CCDC8 peptide forms two hydrogen bonds with Y282 and S280 of ANKRA2 (Figures S6 and S7). These hydrogen bonds and the additional hydrophobic contacts with the N- and C-terminal ends of the CCDC8 peptide (Figure 5; Figures S6 and S7) explain the much stronger ANKRA2-binding affinity for CCDC8 than that for HDAC4 (0.18 versus 1.6 μM, Figures 3 and 4A).

We have recently reported that S350 phosphorylation of HDAC4 decreases the binding (Xu et al., 2012). By contrast, T504 phosphorylation of the CCDC8 peptide only weakened the binding slightly (by ~2.5-fold) (Figure 3). There is no detectable binding between the phosphorylated CCDC8 peptide and 14-3-3γ (Figure 3F), which binds the phosphorylated HDAC4 peptide at a K_d value of 9 μM (Figure 4A) (Xu et al., 2012). Next, we compared the two phosphorylated motifs of HDAC4 and CCDC8 centered at pS350 and pT504, respectively. Sequence comparison indicated that K507 of CCDC8 is at the (i + 3) position, corresponding to the position of N353 of HDAC4 (Figure 4B). The latter has a shorter side chain and forms two hydrogen bonds with 14-3-3 residues (Xu et al., 2012). The side chain of K507 of CCDC8 may cause steric clash with those residues in 14-3-3γ. This conclusion is further supported by the isothermal titration calorimetry (ITC) data that 14-3-3γ binds to the phosphorylated CCDC8 peptide very weakly (Figures 3F and 4A).

Table 1. Parameter Statistics for the Complex Crystal Structure of the Ankyrin-Repeat Domain of ANKRA2 Bound to the CCDC8 Peptide

Space group	$P2_1$
Cell *a*, *b*, *c* (Å), β (°)	38.73, 49.79, 41.24, 98.23
Resolution range (high-resolution shell)[a] (Å)	30.00–1.80 (1.90–1.80)
Number of unique reflections (Friedel)[a]	14,082 (1,988)
Completeness[a] (%)	98.5 (94.8)
R_{sym}[a]	0.047 (0.650)
Mean[a] ($\langle I \rangle / \sigma(I)$)	16.2 (2.1)
Redundancy[a]	3.7 (3.7)
Refinement resolution (Å)	26.15–1.80
Reflections work/free	13368/712
R_{work}/R_{free}	0.196/0.209
Number of atoms/average B factor (Å^2)	
ANKRA2 protein	1246/30.1
CCDC8 peptide	87/37.7
Rmsd bonds (Å)/angles (°)	0.014/1.4
Ramachandran plot favored/outliers (%)	99.4/0.0

Rmsd, root-mean-square deviation.
[a]Values in parentheses correspond to the highest-resolution shells.

CCDC8 Serves as a Scaffold for Interaction with OBSL1, CUL7, and ANKRA2

Having established that the C-terminal PxLPxL motif of CCDC8 mediates the interaction with ANKRA2, we wondered how this might affect CCDC8 association with OBSL1, a novel protein

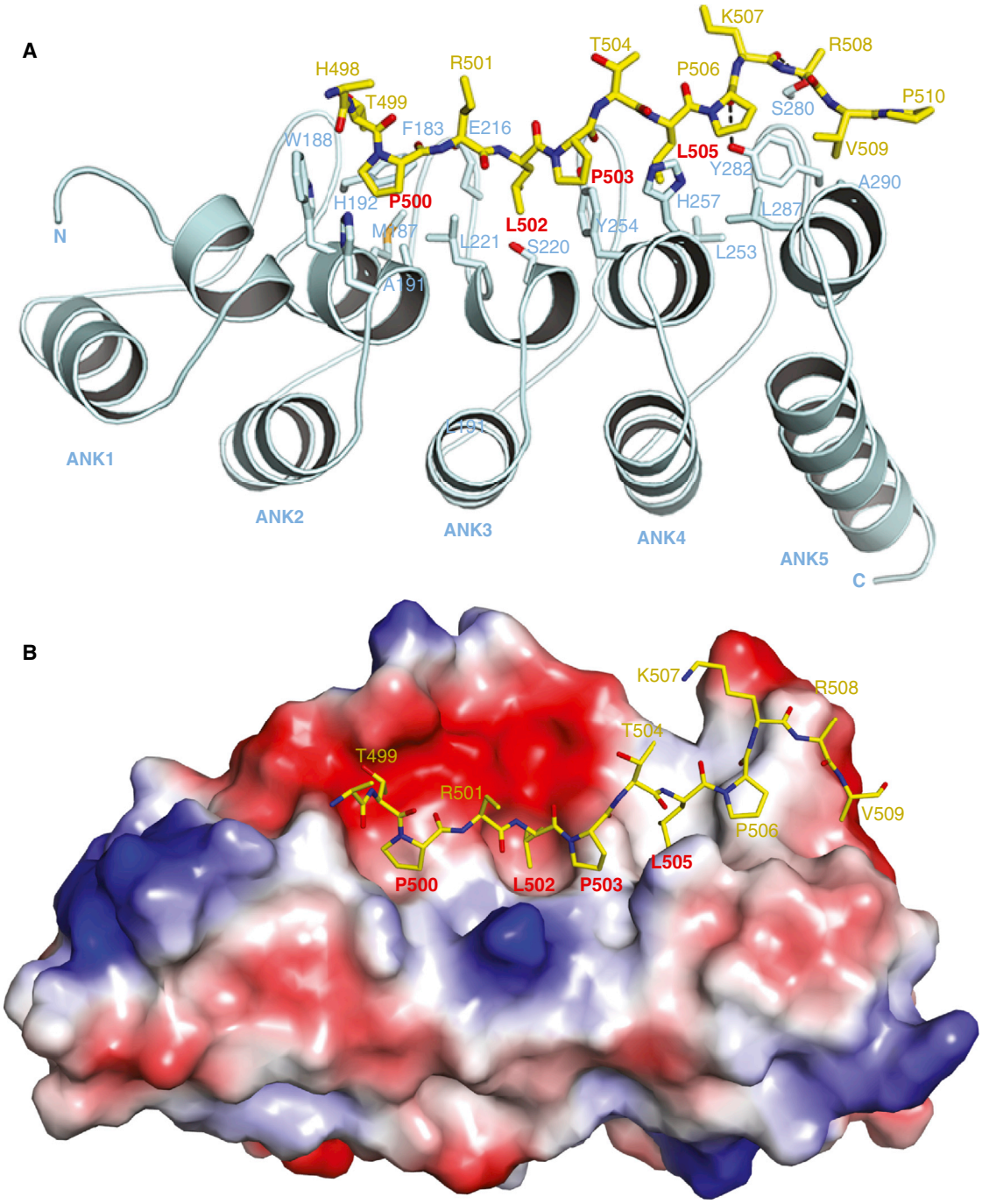

Figure 5. Detailed Atomic Interactions of the Ankyrin Repeats of ANKRA2 with the CCDC8 Peptide

(A) The ankyrin repeats and the CCDC8 peptide are depicted in pale cyan cartoon and yellow sticks, respectively. Residues of ANKRA2 involved in interaction with CCDC8 are shown with sticks. The CCDC8 peptide sequence is the same as listed in Figure 3A.

(B) The ankyrin repeats of ANKRA2 are illustrated in electrostatic surface representation. Key residues of the ANKRA2-binding motif in the CCDC8 peptide are highlighted and labeled in red. See also Figures S6 and S7.

similar to the N-terminal portion of the giant 720-kDa sarcomeric signaling regulator obscurin (Geisler et al., 2007; Hanson et al., 2009), and CUL7, an E3 ubiquitin ligase for p53 and several other proteins (Arai et al., 2003; Dias et al., 2002; Furukawa et al., 2003; Huber et al., 2005; Litterman et al., 2011; Xu et al., 2008). For this, co-IP was performed. OBSL1 coimmunoprecipitated with CCDC8 and enhanced the interaction of CCDC8 with ANKRA2 (Figure 6A, lanes 1–4) and bridged the binding of CCDC8 to CUL7 (lanes 7–8). While an increased amount of CUL7 might have slightly weakened the ANKRA2 binding to CCDC8 (lanes

5–6), an increase in the ANKRA2 amount had minimal impact on CUL7 association with CCDC8 (cf. lanes 5 and 9). The point mutation P503A of CCDC8 disrupted its ability to bind ANKRA2 but exerted no impact on the association with OBSL1 and CUL7 (lanes 10–13), indicating that the C-terminal domain of CCDC8 is important for interaction with ANKRA2 but not OBSL1 and CUL7. In support for this, a CCDC8 mutant lacking the C-terminal domain coprecipitated with OBSL1 and CUL7 (Figure S5C) but not with ANKRA2 (Figure 2C). OBSL1N, an N-terminal fragment corresponding to a mutant encoded in a patient with 3M syndrome (Geisler et al., 2007; Hanson et al., 2009), was sufficient for CCDC8 binding (Figure 6A, lane 14). These results indicate that OBSL1 serves as a scaffold to bridge interaction of CUL7 with CCDC8, which in turn associates with ANKRA2 (Figure 6B). The complex formation among CCDC8, OBSL1, and CUL7 is consistent with a recent report (Yan et al., 2014).

CUL7 is a large protein with multiple domains (Arai et al., 2003; Dias et al., 2002; Furukawa et al., 2003; Xu et al., 2008), so we mapped the domain that mediates interaction with OBSL1 and CCDC8. For this, co-IP was performed, which revealed that the cullin-containing C-terminal portion of CUL7 is necessary and sufficient for association with OBSL1 and CCDC8 (Figure 6C, lanes 5–6 and 12–13). As the cullin domain is responsible for interaction with the RING finger protein ROC1 and for the E3 ubiquitin ligase activity (Arai et al., 2003; Dias et al., 2002; Furukawa et al., 2003; Xu et al., 2008), an interesting possibility is whether the OBSL1/CCDC8 subcomplex competes with ROC1 in binding to the cullin domain. As shown in Figure 6C, ROC1 bound to CUL7 in the presence of expressed OBSL1 and CCDC8 (lanes 1–4 and 8–11), indicating that OBSL1 and CCDC8 do not interfere with ROC1 recruitment to CUL7. Alternatively, two CUL7 populations may form different complexes with OBSL1/CCDC8 and ROC1. Moreover, the C-terminal fragment of CUL7 interacted with ROC1 (lanes 5–7 and 12–14), indicating that the cullin domain possesses sites for simultaneous interaction with the OBSL1/CCDC8 and ROC1/FBXW8 subcomplexes. Interestingly, autoubiquination of the cullin domain appeared to be inhibited by OBSL1 and CCDC8 (Figure 6C, lanes 5–6). Therefore, using its N- and C-terminal domains, CCDC8 serves as a scaffold for interaction with OBSL1 and ANKRA2, respectively, whereas OBSL1 in turn targets CCDC8 to the cullin domain of CUL7 (Figure 6D).

ANKRA2 Inhibits Interaction of CUL7 with HDAC4

As an E3 ubiquitin ligase (Arai et al., 2003; Dias et al., 2002; Furukawa et al., 2003), CUL7 stimulates ubiquitination of p53 (Andrews et al., 2006), insulin receptor substrate (Litterman et al., 2011; Xu et al., 2008), and TBC1D3 (Kong et al., 2012). We thus asked whether ANKRA2 regulates the ligase activity of CUL7 toward these substrates. Cell-based ubiquitination assays failed to detect any effects of ANKRA2 on p53 and TBC1D3 (data not shown), so we wondered whether CUL7 targets unidentified substrates. Because ANKRA2 interacts with the class IIa histone deacetylases (McKinsey et al., 2006; Wang et al., 2005), we investigated whether CUL7 binds to these deacetylases. As shown in Figure 7 (lanes 4, 10, 15, and 21), both HDAC4 and HDAC5 coimmunoprecipitated with CUL7. Interestingly, coexpression of ANKRA2 blocked interaction of CUL7 with both deacetylases (lanes 5, 11, 16, and 22). Strikingly, both were more stable when ANKRA2 was coexpressed (cf. lanes 15 and 21 with lanes 16 and 22, respectively). We also analyzed the mutants I354A and P349A, which contain point mutations at the ANKRA2-binding PxLPxL motif of HDAC4 and disrupt ANKRA2 binding in vitro (data not shown). In the cells, both mutants still interacted with ANKRA2 as efficiently as wild-type HDAC4 (Figure 7, lanes 1–3 and 12–14), indicating that in addition to the PxLPxL motif, HDAC4 contains other sites for ANKRA2 binding, as reported earlier (Wang et al., 2005). Both mutants were slightly less stable than wild-type HDAC4 but were able to bind CUL7 (lanes 4–6 and 15–17). Interestingly, ANKRA2 disrupted the interaction (lanes 7–9 and 18–20). These results indicate that ANKRA2 binds HDAC4 to block its access by CUL7.

DISCUSSION

This study uncovers a link of the ankyrin-repeat protein ANKRA2 to CCDC8, OBSL1, and CUL7 (Figure 8), thereby shedding light on the molecular mechanisms underlying the pathogenesis of 3M syndrome, a unique form of primordial dwarfism (Clayton et al., 2012; Klingseisen and Jackson, 2011). The proteomic survey identified CCDC8 as a major partner of ANKRA2 (Figure 1B). The PxLPxL motif of CCDC8 is necessary and sufficient for the association (Figures 2 and 3). At the sequence level, this motif is more similar to those of HDAC4, megalin, and RFX7 than to that of RFX5 (Figure 4B). Indeed, the motif mediates interaction with ANKRA2 but not with RFXANK (Figure 3). The CCDC8 affinity for ANKRA2 is even higher than that of HDAC4, megalin, or RFX7 (Figure 4A), explaining why CCDC8 was recovered as the top partner of ANKRA2 (Figure 1B). The atomic interactions are highly similar to those in structures of the ANKRA2 complexes with the HDAC4, megalin, and RFX7 peptides (Figure 5; Figures S6 and S7), but CCDC8 also possesses extra contacts with ANKRA2 (Figure S7), making the binding affinity higher than that for HDAC4, megalin, or RFX7 (Figure 4A). Therefore, in addition to the core motif PxLPxL/I, exact sequences within the motif and surrounding regions are important for optimal interaction with ANKRA2 and RFXANK.

While the PxLPxL motif of CCDC8 is located at its C-terminal domain (Figure 4), OBSL1 targets the N-terminal domain to promote the interaction with the CUL7 ligase (Figure 8). CUL7 stimulates ubiquitination of p53, insulin receptor substrate 1, and the hominoid-specific TBC1D3 oncoprotein (Andrews et al., 2006; Kong et al., 2012; Xu et al., 2008). Related to the interaction of CUL7 with p53, CCDC8 was recently reported to bind p53 (Dai et al., 2011). Our results indicate that ANKRA2 does not affect p53 ubiquitination (data not shown). Instead, we found that ANKRA2 blocks CUL7 interaction with HDAC4/5 and perhaps also the other two class IIa deacetylases (Figure 7) (Yang and Seto, 2008).

The *CCDC8*, *CUL7*, and *OBSL1* genes are mutated in patients with 3M syndrome (Al-Dosari et al., 2012; Hanson et al., 2011). The unexpected identification of CCDC8 as a major partner of ANKRA2 (Figure 1B) suggests an important role of ANKRA2 in 3M syndrome. Whether the gene is mutated in the patients lacking mutations in the *CUL7*, *OBSL1*, and *CCDC8* genes is an interesting possibility worth consideration. ANKRA2 may also modify the outcome in patients who carry mutations in the *CUL7*, *OBSL1*, and *CCDC8* genes. In addition to short stature,

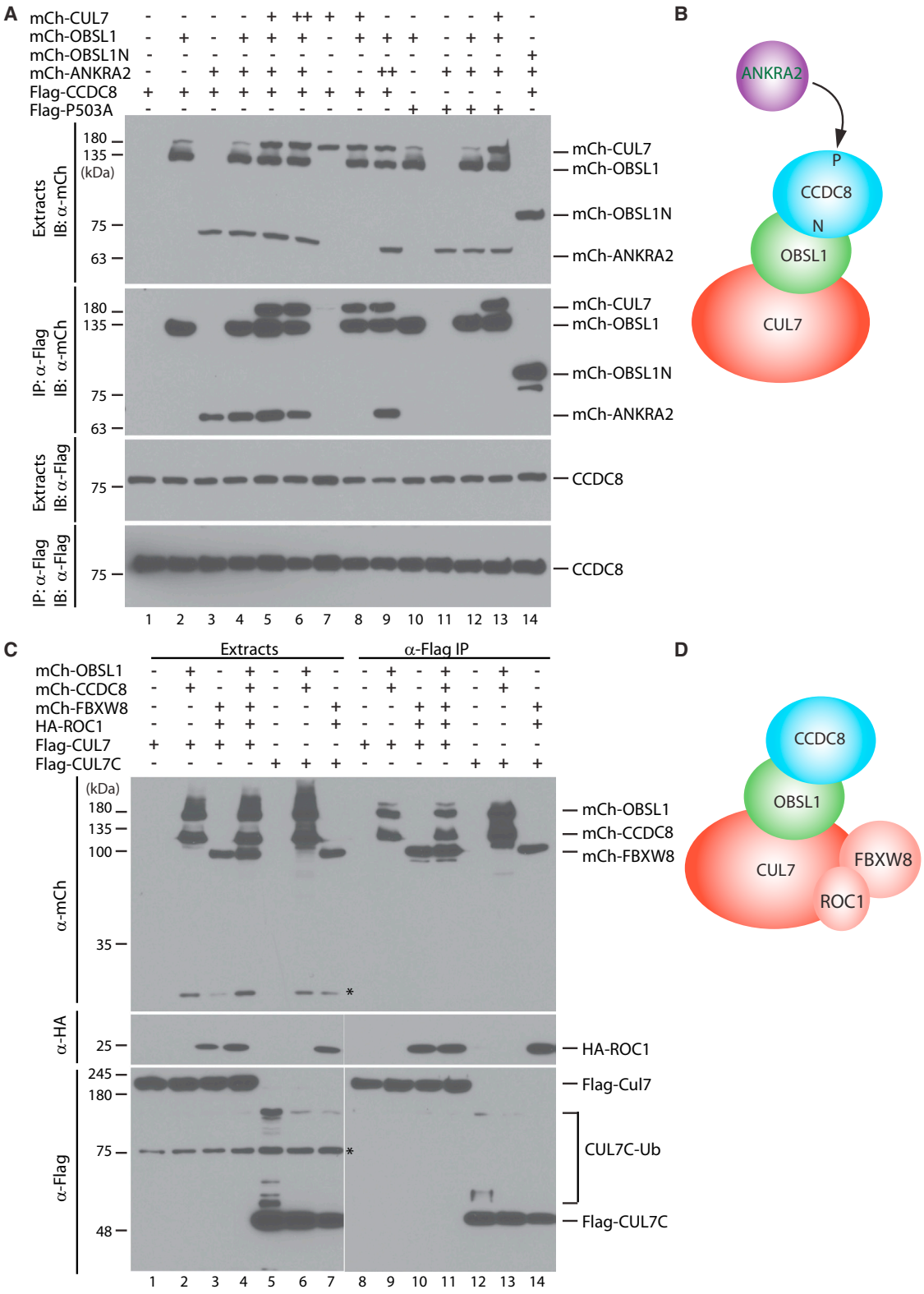

Figure 6. OBSL1 Promotes the Interaction of CCDC8 with CUL7 and ANKRA2

(A) Expression vectors for the indicated mCherry (mCh) fusion proteins were transfected into HEK293 cells along with the expression plasmid for Flag-tagged CCDC8 or its point mutant P503A. Soluble extracts were prepared for affinity purification and immunoblotting.

(B) Cartoon illustrating that OBSL1 mediates interaction of CUL7 with CUL7 to the N-terminal domain (N) whereas ANKRA2 binds to the PxLPxL motif located at the C-terminal domain (P).

(legend continued on next page)

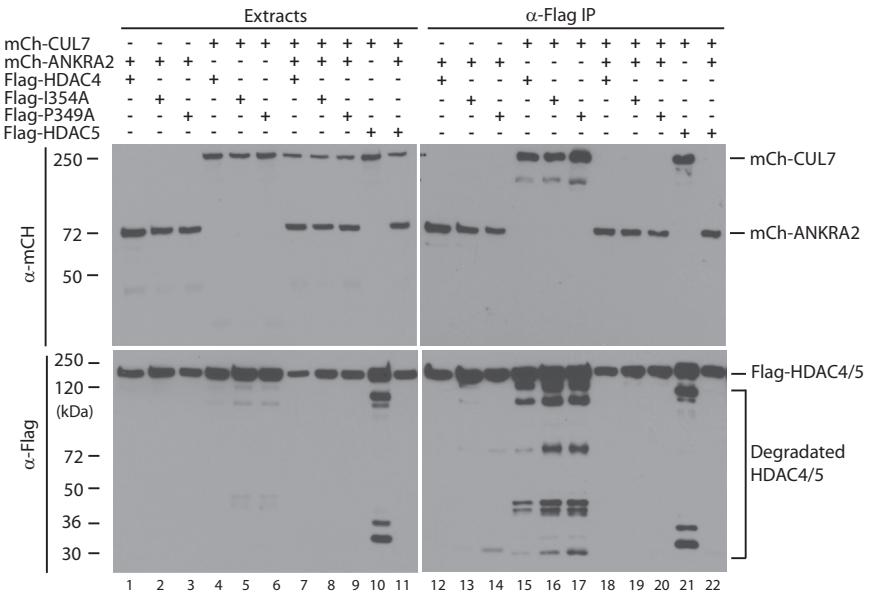

Figure 7. ANKRA2 Inhibits Interaction of CUL7 with HDAC4 and HDAC5

Expression vectors for mCh tagged CUL7 and ANKRA2 were separately or simultaneously transfected into HEK293 cells along with the expression plasmid for Flag-tagged HDAC4, two point mutants, and HDAC5 as indicated. Soluble extracts were prepared for affinity purification and immunoblotting. The point mutants P349A and I354A contain mutations replacing the key residues P349 and I354, respectively, within the ANKRA2-binding PxLPxL motif of HDAC4 with alanine and display minimal ANKRA2 binding in vitro (data not shown), but both mutants still interact with ANKRA2 efficiently in HEK293 cells. Thus, in the cells, HDAC4 contains multiple ANKRA2-binding sites as reported earlier (Wang et al., 2005).

patients with 3M syndrome display unusual facial features and skeletal abnormalities (Clayton et al., 2012; Hanson et al., 2011, 2012; Litterman et al., 2011). ANKRA2 impairs CUL7 binding to HDAC4 (Figure 7). Haploinsufficiency of the *HDAC4* gene leads to craniofacial and skeletal abnormalities (Williams et al., 2010), and the mouse ortholog is crucial for skeletal development (Vega et al., 2004). 3M syndrome is underdiagnosed (Al-Dosari et al., 2012) and displays similarity to other primordial growth disorders, such as Yakut short-stature syndrome (Maksimova et al., 2007) and Silver-Russell syndrome (Akawi et al., 2011). Thus, the unexpected molecular link uncovered herein provides an important lead about the mechanisms underlying 3M syndrome and other primordial dwarfism.

While RFXANK forms a trimeric transcription factor complex with RFX5 and RFXAP to recruit the coactivator CIITA for regulating gene expression programs that are affected in BLS patients (Reith and Mach, 2001; Ting and Trowsdale, 2002), the biological function of ANKRA2 remains unclear. Its high sequence similarity to RFXANK (Figure 1A; Figure S1) suggests that ANKRA2 plays a similar role in vivo. However, unlike the RFXANK, RFX5, RFXAP, and CIITA genes, the *ANKRA2* gene has never been recovered as one mutated in BLS patients (Reith and Mach, 2001; Ting and Trowsdale, 2002). Related to this, only ANKRA2 was identified as the partner of megalin, HDAC4, and HDAC5 in yeast two-hybrid screening of different libraries (McKinsey et al., 2006; Rader et al., 2000; Wang et al., 2005). Thus, there are functional differences between ANKRA2 and RFXANK, even although they behave similarly in cell-based assays (Krawczyk et al., 2005; Long and Boss, 2005; McKinsey et al., 2006; Wang et al., 2005). In support of this, recent quantitative binding and crystal structural analyses showed that one key residue (H257 of ANKRA2 and R199 of RFXANK, Figure S1) plays a dominant role in dictating specificity in partner selection (Xu et al., 2012). The proteomic survey presented herein reiterates the functional similarity and difference between ANKRA2 and RFXANK (Figure 1B; Tables S1 and S2). As expected from the published studies (Krawczyk et al., 2005; Long and Boss, 2005), RFXANK and ANKRA2 coprecipitated with RFX5 and RFXAP. While RFX5 was recovered as the top partner of RFXANK, CCDC8 was identified as the major partner of ANKRA2 (Figure 1B; Table S1). In contrast, CCDC8 did not copurify with RFXANK, supporting that RFXANK and ANKRA2 have different targets and functions in vivo (Figure 1C). Of relevance, histones H3.1 and H3.3 are almost identical (sequence identity >95%), but their targets and functions are different in vivo (Goldberg et al., 2010).

RFX7 is ranked the second in purifications for both baits (Figure 1B; Tables S1 and S2). This is a novel protein linked to breast cancer and neural tube development (Aftab et al., 2008; Bae et al., 2014; Manojlovic et al., 2014; Yau et al., 2010), RFX7 displays significant similarity in its putative DNA binding domain with the RFX domain of RFX5 (Figure S3). Within this domain is a PxLPxL motif. However, the motif is more similar to those of HDAC4 and megalin than to that of RFX5 (Figure 4; Figure S3). In particular, P175 of RFX5, a key residue making it preferable for RFXANK binding (Xu et al., 2012), is not conserved in RFX7. Thus, RFX7 prefers ANKRA2 over RFXANK (Figure 4; Figure S7). The *Drosophila* homolog is more similar to RFX7 than RFX5 (Figure S3), and there are no apparent RFXAP homologs in the fly, suggesting that the RFX7-ANKRA2 link is conserved from flies to humans.

Among the proteins copurified with RFXANK and ANKRA2, CCDC8, RFX7, and HDAC5 are the only three containing conserved PxLPxL/I motifs (Figure 1B; Tables S1 and S2), so the interesting question is how the other partners such as the ubiquitin E3 ligase HUWE1 and the uncharacterized protein

(C) Expression vectors for HA-ROC1 and the indicated mCh fusion proteins were transfected into HEK293 cells along with the expression plasmid for Flag-tagged CUL7 or its truncation mutant containing the C-terminal cullin domain. Soluble extracts were prepared for affinity purification and immunoblotting. Asterisks denote nonspecific bands.

(D) Cartoon illustrating interaction of the C-terminal cullin domain CUL7 with the OBSL1/CCDC8 and ROC1/FBXW8 subcomplexes. See also Figure S5C.

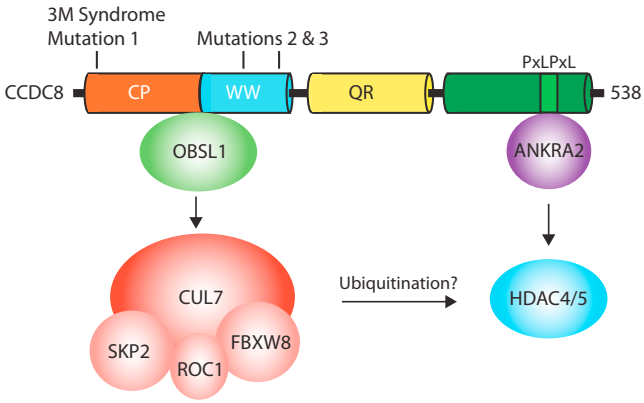

Figure 8. Model Explaining How ANKRA2 Interacts with CCDC8 and May Regulate Functions of HDAC4/5 and RFX7

Acting as a multidomain scaffold, CCDC8 uses the N-terminal part (composed of the uncharacterized CP and WW domains) for binding to OBSL1, with in turn recruits the CUL7 ubiquitin ligase complex for regulating ubiquitination of its substrates. The C-terminal region of CCDC8 is required for interaction with ANKRA2 and also for an unidentified factor (not illustrated). The suggestion for this unidentified factor is based on the observation that the entire C-terminal region is highly conserved from mouse to humans (Figure S4) and the PxLPxL motif is embedded within this region. ANKRA2 binds to the PxLPxL motif of CCDC8 and inhibits interaction of CUL7 with (and perhaps also ubiquitination of) HDAC4/5 and RFX7. Structural domains of CCDC8 are illustrated and labeled as in Figure 2A. Three 3M syndrome-causing mutations are located at the coding sequence for the N-terminal portion of CCDC8 and are expected to result in expression of aberrant proteins to disrupt the network formed with CUL7, OBSL1, and ANKRA2. See also Figure S7.

C20orf117 (Figure 1B) may interact with ANKRA2 and RFXANK. One possibility is that the interaction is facilitated or mediated by others. For example, RFX5 facilitates RFXANK association with RFXAP, and CCDC8 bridges interaction of CUL7, OBSL1, and FBXW8 with ANKRA2 (Figure 1C). Another possibility is that some of the associated proteins directly interact with ANKRA2 and RFXANK in a manner independent of PxLPxL/I motifs.

In summary, proteomic analysis of proteins interacting with the two paralogous ankyrin-repeat proteins ANKRA2 and RFXANK has uncovered two groups of proteins with genes that are mutated in 3M syndrome and BLS. ANKRA2 recognizes a conserved PxLPxL motif on the eutherian-specific protein CCDC8, which in turn interacts with the cytoskeletal protein OBSL1 and the ubiquitin ligase CUL7 (Figure 8). Functionally, ANKRA2 inhibits CUL7 interaction with HDAC4/5 (Figure 8). How CUL7-mediated ubiquitination is involved in the regulation is an interesting question awaiting further investigation (Figure 8).

EXPERIMENTAL PROCEDURES

Protein Expression in Mammalian Cells and Affinity Protein Purification

We expressed ANKRA2 and RFXANK as GFP-tagged fusion proteins in human embryonic kidney (HEK) 293 cells. The GFP fusion tag was not only to detect and visualize the protein expression but also to take advantage of the high specificity and low background of GFP-Trap affinity beads developed from a unique camel single-chain antibody (Allele Biotechnology and ChromoTek) (Rothbauer et al., 2008). The GFP fusion proteins were affinity purified on the beads and specifically associated proteins were analyzed by mass spectrometry. This procedure is commonly referred to as IP-MS, in which the relative abundance of each interacting protein is reflected in their total spectrum counts of the resulting tryptic peptides (Figure 1B; Table S1).

Bacterial Protein Expression, Purification, and Crystallization

Preparation of human ANKRA2 ankyrin repeats was performed as described (Xu et al., 2012). For crystallization, the purified ANKRA2 protein was mixed with the CCDC8 peptide corresponding to residues 494–510 at a ratio of 1:2, and crystals of the complex were obtained with the hanging-drop vapor diffusion method at 18°C in a crystallization buffer containing 0.1 M HEPES (pH 7.5), 0.2 M NaCl, and 25% PEG 3350. The crystals were frozen in liquid nitrogen without cryoprotectants.

Collection and Analysis of Crystal Structural Data

Three hundred and sixty half-degree oscillation images, collected on a copper-rotating anode equipped with an image plate detector (Rigaku FR-E and Raxis-IV-HTC, respectively), were reduced using the XDS program (Kabsch, 2010). Reflections were scaled using POINTLESS/SCALA (Evans, 2006) and converted to structure factor amplitudes with TRUNCATE (French and Wilson, 1978). The structure was solved by molecular replacement with the published coordinates from the PDB entry 3SO8 and the program PHASER (McCoy et al., 2007). The model was rebuilt, refined, and validated in several iterations, respectively, using COOT (Emsley et al., 2010), REFMAC (Murshudov et al., 2011), and the MOLPROBITY server (Chen et al., 2010).

ITC

ITC measurements were recorded at 25°C using a VP-ITC microcalorimeter (MicroCal) as described (Xu et al., 2012). To determine the K_d value of CCDC8 binding to ANKRA2, 10 μl of the peptide solution (residues 494–510 of CCDC8, Figure 4B; 1.0 mM) was injected into a sample cell containing 40 or 80 μM of the ANKRA2 ankyrin-repeat fragment (residues 142–313) in 20 mM Tris-HCl (pH 7.5) and 150 mM NaCl. For binding to RFXANK, 10 μl of the CCDC8 peptide solution (0.5 mM) was injected into a sample cell containing 35 μM of the RFXANK ankyrin-repeat fragment (residues 90–260). For binding to 14-3-3, 10 μl of the pT504 CCDC8 peptide solution (Figure 4B, 1.0 mM) was injected into a sample cell containing 50 μM of 14-3-3γ. For RFX7 binding to ANKRA2, 10 μl of the RFX7 peptide solution (Figure 4B, 1.0 mM) was injected into a sample cell containing 50 μM of the ANKRA2 fragment. For binding to ANKRA2, 10 μl of the RFX7 peptide solution (2.0 mM) was injected into a sample cell containing 100 μM of the ANKRA2 fragment. The concentrations of protein and peptide were estimated with absorbance spectroscopy using the extinction coefficients. A total of 25 injections were performed with an interval of 180 s and a reference power of 15 μcal/s. Binding isotherms were plotted using a one-site binding model analyzed by Origin Software (MicroCal).

Co-IP

HEK293 cells were seeded in 6-cm dishes at 0.5 × 10^6 cells per dish and transiently transfected with the expression plasmids for Flag-tagged CCDC8 or its mutants along expressing plasmids for GFP-ANKRA2, GFP-tagged ANKRA2 point mutants, and GFP-RFXANK as indicated. Two days post transfection, the cells were washed twice with PBS and lysed in situ with 0.1 ml of cold buffer K for preparation of soluble extracts as described (Ullah et al., 2008). Co-IP was performed with anti-Flag M2 agarose (Sigma) and specifically bound proteins were eluted with FLAG peptide (Sigma) for immunoblotting with anti-FLAG (Sigma, clone M2), anti-GFP (Santa Cruz Biotech, B-2, sc-9996), and anti-mCherry (BioVision, 5993-100) antibodies as specified.

Additional experimental procedures are included in the Supplemental Information.

ACCESSION NUMBERS

Atomic coordinates for the ANKRA2 complex structures with the CCDC8, RFX7, HDAC4, and megalin peptides have been deposited in PDB under the entry codes 4LG6, 4QQI, 3V31, and 3V2X, respectively.

SUPPLEMENTAL INFORMATION

Supplemental Information includes Supplemental Experimental Procedures, seven figures, and two tables and can be found with this article online at http://dx.doi.org/10.1016/j.str.2015.02.001.

AUTHOR CONTRIBUTIONS

J.N. initiated the project and verified the interaction of ANKRA2 with the PxLPxL motif of CCDC8; C.X. and W.T. carried out X-ray crystallography and structural determination; C.X. performed the ITC experiments and analyzed the data; J.J. and V.N. carried out mass spectrometry; J.N. and J.A.A. determined the interaction of CCDC8 with OBSL1 and CUL7; J.A.A. analyzed the interaction of HDAC4/5 with CUL7 and ANKRA2; L.Y. and R.W. provided reagents; X.J.Y., J.M., and T.P. supervised the project; X.J.Y, J.M., C.X., and J.J. wrote the manuscript.

ACKNOWLEDGMENTS

This research was supported by operating grants from the Canadian Institutes for Health Research (CIHR, to X.J.Y. and T.P.), as well as by the Structural Genomics Consortium, a registered charity that received funds from the CIHR, the Canadian Foundation for Innovation, Genome Canada through the Ontario Genomics Institute, GlaxoSmithKline, Karolinska Institute, the Knut and Alice Wallenberg Foundation, the Ontario Innovation Trust, the Ontario Ministry for Research and Innovation, Merck & Co., Inc., the Novartis Research Foundation, the Swedish Agency for Innovation Systems, the Swedish Foundation for Strategic Research and the Wellcome Trust.

Received: December 3, 2014
Revised: February 2, 2015
Accepted: February 3, 2015
Published: March 5, 2015

REFERENCES

Aftab, S., Semenec, L., Chu, J.S., and Chen, N. (2008). Identification and characterization of novel human tissue-specific RFX transcription factors. BMC Evol. Biol. *8*, 226.

Akawi, N.A., Ali, B.R., Hamamy, H., Al-Hadidy, A., and Al-Gazali, L. (2011). Is autosomal recessive Silver-Russel syndrome a separate entity or is it part of the 3-M syndrome spectrum? Am. J. Med. Genet. A *155A*, 1236–1245.

Al-Dosari, M.S., Al-Shammari, M., Shaheen, R., Faqeih, E., Alghofely, M.A., Boukai, A., and Alkuraya, F.S. (2012). 3M syndrome: an easily recognizable yet underdiagnosed cause of proportionate short stature. J. Pediatr. *161*, 139.e1–145.e1.

Andrews, P., He, Y.J., and Xiong, Y. (2006). Cytoplasmic localized ubiquitin ligase cullin 7 binds to p53 and promotes cell growth by antagonizing p53 function. Oncogene *25*, 4534–4548.

Arai, T., Kasper, J.S., Skaar, J.R., Ali, S.H., Takahashi, C., and DeCaprio, J.A. (2003). Targeted disruption of p185/Cul7 gene results in abnormal vascular morphogenesis. Proc. Natl. Acad. Sci. USA *100*, 9855–9860.

Bae, B., Tietjen, I., Atabay, K.D., Evrony, G.D., Johnson, M.B., Asare, E., Wang, P.P., Murayama, A.Y., Im, K., Lisgo, S.N., et al. (2014). Evolutionarily dynamic alternative splicing of GPR56 regulates regional cerebral cortical patterning. Science *343*, 746–768.

Chen, H.L., and D'Mello, S.R. (2010). Induction of neuronal cell death by paraneoplastic Ma1 antigen. J. Neurosci. Res. *88*, 3508–3519.

Chen, V.B., Arendall, W.B., 3rd, Headd, J.J., Keedy, D.A., Immormino, R.M., Kapral, G.J., Murray, L.W., Richardson, J.S., and Richardson, D.C. (2010). MolProbity: all-atom structure validation for macromolecular crystallography. Acta Crystallogr. D Biol. Crystallogr. *66*, 12–21.

Christensen, E.I., and Birn, H. (2002). Megalin and cubilin: multifunctional endocytic receptors. Nat. Rev. Mol. Cell Biol. *3*, 256–266.

Clayton, P.E., Hanson, D., Magee, L., Murray, P.G., Saunders, E., Abu-Amero, S.N., Moore, G.E., and Black, G.C. (2012). Exploring the spectrum of 3-M syndrome, a primordial short stature disorder of disrupted ubiquitination. Clin. Endocrinol. (Oxf) *77*, 335–342.

Dai, C., Tang, Y., Jung, S.Y., Qin, J., Aaronson, S.A., and Gu, W. (2011). Differential effects on p53-mediated cell cycle arrest vs. apoptosis by p90. Proc. Natl. Acad. Sci. USA *108*, 18937–18942.

Dias, D.C., Dolios, G., Wang, R., and Pan, Z.Q. (2002). CUL7: a DOC domain-containing cullin selectively binds Skp1.Fbx29 to form an SCF-like complex. Proc. Natl. Acad. Sci. USA *99*, 16601–16606.

Emsley, P., Lohkamp, B., Scott, W.G., and Cowtan, K. (2010). Features and development of Coot. Acta Crystallogr. D Biol. Crystallogr. *66*, 486–501.

Evans, P. (2006). Scaling and assessment of data quality. Acta Crystallogr. D Biol. Crystallogr. *62*, 72–82.

French, S., and Wilson, K. (1978). Treatment of negative intensity observations. Acta Crystallogr. A *34*, 517–525.

Furukawa, M., He, Y.J., Borchers, C., and Xiong, Y. (2003). Targeting of protein ubiquitination by BTB-Cullin 3-Roc1 ubiquitin ligases. Nat. Cell Biol. *5*, 1001–1007.

Geisler, S.B., Robinson, D., Hauringa, M., Raeker, M.O., Borisov, A.B., Westfall, M.V., and Russell, M.W. (2007). Obscurin-like 1, OBSL1, is a novel cytoskeletal protein related to obscurin. Genomics *89*, 521–531.

Goldberg, A.D., Banaszynski, L.A., Noh, K.M., Lewis, P.W., Elsaesser, S.J., Stadler, S., Dewell, S., Law, M., Guo, X., Li, X., et al. (2010). Distinct factors control histone variant H3.3 localization at specific genomic regions. Cell *140*, 678–691.

Hanson, D., Murray, P.G., Sud, A., Temtamy, S.A., Aglan, M., Superti-Furga, A., Holder, S.E., Urquhart, J., Hilton, E., Manson, F.D., et al. (2009). The primordial growth disorder 3-M syndrome connects ubiquitination to the cytoskeletal adaptor OBSL1. Am. J. Hum. Genet. *84*, 801–806.

Hanson, D., Murray, P.G., O'Sullivan, J., Urquhart, J., Daly, S., Bhaskar, S.S., Biesecker, L.G., Skae, M., Smith, C., Cole, T., et al. (2011). Exome sequencing identifies CCDC8 mutations in 3-M syndrome, suggesting that CCDC8 contributes in a pathway with CUL7 and OBSL1 to control human growth. Am. J. Hum. Genet. *89*, 148–153.

Hanson, D., Murray, P.G., Coulson, T., Sud, A., Omokanye, A., Stratta, E., Sakhinia, F., Bonshek, C., Wilson, L.C., Wakeling, E., et al. (2012). Mutations in CUL7, OBSL1 and CCDC8 in 3-M syndrome lead to disordered growth factor signalling. J. Mol. Endocrinol. *49*, 267–275.

Huber, C., Dias-Santagata, D., Glaser, A., O'Sullivan, J., Brauner, R., Wu, K., Xu, X., Pearce, K., Wang, R., Uzielli, M.L., et al. (2005). Identification of mutations in CUL7 in 3-M syndrome. Nat. Genet. *37*, 1119–1124.

Kabsch, W. (2010). Xds. Acta Crystallogr. D Biol. Crystallogr. *66*, 125–132.

Klingseisen, A., and Jackson, A.P. (2011). Mechanisms and pathways of growth failure in primordial dwarfism. Genes Dev. *25*, 2011–2024.

Kong, C., Samovski, D., Srikanth, P., Wainszelbaum, M.J., Charron, A.J., Liu, J., Lange, J.J., Chen, P.I., Pan, Z.Q., Su, X., et al. (2012). Ubiquitination and degradation of the hominoid-specific oncoprotein TBC1D3 is mediated by CUL7 E3 ligase. PLoS One *7*, e46485.

Krawczyk, M., Masternak, K., Zufferey, M., Barras, E., and Reith, W. (2005). New functions of the major histocompatibility complex class II-specific transcription factor RFXANK revealed by a high-resolution mutagenesis study. Mol. Cell. Biol. *25*, 8607–8618.

Lin, J.H., Makris, A., McMahon, C., Bear, S.E., Patriotis, C., Prasad, V.R., Brent, R., Golemis, E.A., and Tsichlis, P.N. (1999). The ankyrin repeat-containing adaptor protein Tvl-1 is a novel substrate and regulator of Raf-1. J. Biol. Chem. *274*, 14706–14715.

Litterman, N., Ikeuchi, Y., Gallardo, G., O'Connell, B.C., Sowa, M.E., Gygi, S.P., Harper, J.W., and Bonni, A. (2011). An OBSL1-Cul7Fbxw8 ubiquitin ligase signaling mechanism regulates Golgi morphology and dendrite patterning. PLoS Biol. *9*, e1001060.

Long, A.B., and Boss, J.M. (2005). Evolutionary conservation and characterization of the bare lymphocyte syndrome transcription factor RFX-B and its paralogue ANKRA2. Immunogenetics *56*, 788–797.

Maksimova, N., Hara, K., Miyashia, A., Nikolaeva, I., Shiga, A., Nogovicina, A., Sukhomyasova, A., Argunov, V., Shvedova, A., Ikeuchi, T., et al. (2007).

Clinical, molecular and histopathological features of short stature syndrome with novel CUL7 mutation in Yakuts: new population isolate in Asia. J. Med. Genet. *44*, 772–778.

Manojlovic, Z., Earwood, R., Kato, A., Stefanovic, B., and Kato, Y. (2014). RFX7 is required for the formation of cilia in the neural tube. Mech. Dev. *132*, 28–37.

Masternak, K., Barras, E., Zufferey, M., Conrad, B., Corthals, G., Aebersold, R., Sanchez, J.C., Hochstrasser, D.F., Mach, B., and Reith, W. (1998). A gene encoding a novel RFX-associated transactivator is mutated in the majority of MHC class II deficiency patients. Nat. Genet. *20*, 273–277.

McCoy, A.J., Grosse-Kunstleve, R.W., Adams, P.D., Winn, M.D., Storoni, L.C., and Read, R.J. (2007). Phaser crystallographic software. J. Appl. Crystallogr. *40*, 658–674.

McKinsey, T.A., Kuwahara, K., Bezprozvannaya, S., and Olson, E.N. (2006). Class II histone deacetylases confer signal responsiveness to the ankyrin-repeat proteins ANKRA2 and RFXANK. Mol. Biol. Cell *17*, 438–447.

Miller, J.D., McKusick, V.A., Malvaux, P., Temtamy, S., and Salinas, C. (1975). The 3-M syndrome: a heritable low birthweight dwarfism. Birth Defects Orig. Artic. Ser. *11*, 39–47.

Murshudov, G.N., Skubak, P., Lebedev, A.A., Pannu, N.S., Steiner, R.A., Nicholls, R.A., Winn, M.D., Long, F., and Vagin, A.A. (2011). REFMAC5 for the refinement of macromolecular crystal structures. Acta Crystallogr. D Biol. Crystallogr. *67*, 355–367.

Nagarajan, U.M., Louis-Plence, P., DeSandro, A., Nilsen, R., Bushey, A., and Boss, J.M. (1999). RFX-B is the gene responsible for the most common cause of the bare lymphocyte syndrome, an MHC class II immunodeficiency. Immunity *10*, 153–162.

Rader, K., Orlando, R.A., Lou, X., and Farquhar, M.G. (2000). Characterization of ANKRA, a novel ankyrin repeat protein that interacts with the cytoplasmic domain of megalin. J. Am. Soc. Nephrol. *11*, 2167–2178.

Reith, W., and Mach, B. (2001). The bare lymphocyte syndrome and the regulation of MHC expression. Annu. Rev. Immunol. *19*, 331–373.

Rothbauer, U., Zolghadr, K., Muyldermans, S., Schepers, A., Cardoso, M.C., and Leonhardt, H. (2008). A versatile nanotrap for biochemical and functional studies with fluorescent fusion proteins. Mol. Cell. Proteomics *7*, 282–289.

Schuller, M., Jenne, D., and Voltz, R. (2005). The human PNMA family: novel neuronal proteins implicated in paraneoplastic neurological disease. J. Neuroimmunol. *169*, 172–176.

Ting, J.P., and Trowsdale, J. (2002). Genetic control of MHC class II expression. Cell *109*, S21–S33.

Ullah, M., Pelletier, N., Xiao, L., Zhao, S.P., Wang, K., Degerny, C., Tahmasebi, S., Cayrou, C., Doyon, Y., Goh, S.L., et al. (2008). Molecular architecture of quartet MOZ/MORF histone acetyltransferase complexes. Mol. Cell. Biol. *28*, 6828–6843.

Vega, R.B., Matsuda, K., Oh, J., Barbosa, A.C., Yang, X., Meadows, E., McAnally, J., Pomajzl, C., Shelton, J.M., Richardson, J.A., et al. (2004). Histone deacetylase 4 controls chondrocyte hypertrophy during skeletogenesis. Cell *119*, 555–566.

Wang, A.H., Gregoire, S., Zika, E., Xiao, L., Li, C.S., Li, H., Wright, K.L., Ting, J.P., and Yang, X.J. (2005). Identification of the ankyrin repeat proteins ANKRA and RFXANK as novel partners of class IIa histone deacetylases. J. Biol. Chem. *280*, 29117–29127.

Wang, H., Chen, Y., Lin, P., Li, L., Zhou, G., Liu, G., Logsdon, C., Jin, J., Abbruzzese, J.L., and Tan, T.H. (2014). The CUL7/F-box and WD repeat domain containing 8 (CUL7/Fbxw8) ubiquitin ligase promotes degradation of hematopoietic progenitor kinase 1. J. Biol. Chem. *289*, 4009–4017.

Williams, S.R., Aldred, M.A., Der Kaloustian, V.M., Halal, F., Gowans, G., McLeod, D.R., Zondag, S., Toriello, H.V., Magenis, R.E., and Elsea, S.H. (2010). Haploinsufficiency of HDAC4 causes brachydactyly mental retardation syndrome, with brachydactyly type E, developmental delays, and behavioral problems. Am. J. Hum. Genet. *87*, 219–228.

Xu, X., Sarikas, A., Dias-Santagata, D.C., Dolios, G., Lafontant, P.J., Tsai, S.C., Zhu, W., Nakajima, H., Nakajima, H.O., Field, L.J., et al. (2008). The CUL7 E3 ubiquitin ligase targets insulin receptor substrate 1 for ubiquitin-dependent degradation. Mol. Cell *30*, 403–414.

Xu, C., Jin, J., Bian, C., Lam, R., Tian, R., Weist, R., You, L., Nie, J., Bochkarev, A., Tempel, W., et al. (2012). Sequence-specific recognition of a PxLPxI/L motif by an ankyrin repeat tumbler lock. Sci. Signal. *5*, ra39.

Yan, J., Yan, F., Li, Z., Sinnott, B., Cappell, K.M., Yu, Y., Mo, J., Duncan, J.A., Chen, X., Cormier-Daire, V., et al. (2014). The 3M complex maintains microtubule and genome integrity. Mol. Cell *54*, 791–804.

Yang, X.J., and Seto, E. (2008). The Rpd3/Hda1 family of lysine deacetylases: from bacteria and yeast to mice and men. Nat. Rev. Mol. Cell Biol. *9*, 206–218.

Yau, C., Esserman, L., Moore, D.H., Waldman, F., Sninsky, J., and Benz, C.C. (2010). A multigene predictor of metastatic outcome in early stage hormone receptor-negative and triple-negative breast cancer. Breast Cancer Res. *12*, R85.

